Proceedings of the 30th International Cosmic Ray Conference
Rogelio Caballero, Juan Carlos D'Olivo,
Gustavo Medina-Tanco, José F. Valdés-Galicia (eds.)
Universidad Nacional Autonóma de México,
Mexico City, Mexico, 2009
Vol. 6, pages 359-378

30TH INTERNATIONAL COSMIC RAY CONFERENCE

Hadronic Interactions and Cosmic Ray Particle Physics

RALPH ENGEL
Institut für Kernphysik, Forschungszentrum Karlsruhe, Postfach 3640, 76021 Karlsruhe, Germany
Ralph.Engel@ik.fzk.de

Abstract. This article is a summary of contributions to the International Cosmic Ray Conference 2007 presented mainly in the sessions HE 1.6 *(EAS Simulations)* and HE 3.1 - 3.5 *(Interactions, Particle Physics Aspects, Astroparticle Physics and Cosmology)*. Emphasis is put on a discussion of these contributions within the context of the overall status of the field rather than on a more complete presentation of the individual contributions.

Introduction

On one hand, cosmic rays provide a particle beam that can be used for studies of particle interaction and multiparticle production, or searches for new physics by measuring air showers or secondary particle fluxes. On the other hand, a good understanding of particle interaction is needed for interpreting the measured data in terms of, for example, primary particle energy distributions, elemental composition, or physics beyond the Standard Model. This interrelation between cosmic ray and particle physics is the embracing theme of the contributions to the sessions HE 1.6 *(EAS Simulations)* and HE 3.1 - 3.5 *(Interactions, Particle Physics Aspects, Astroparticle Physics and Cosmology)* of the International Cosmic Ray Conference in Merida. The following article is a write-up of the rapporteur talk of these sessions and an attempt to discuss the corresponding contributions within the broad astroparticle and particle physics context. A presentation of all individual contributions would be impossible and is clearly beyond the scope of this work.

The topics discussed in the sessions HE 1.6 and 3.1 - 3.5 can roughly be subdivided into (i) theoretical, phenomenological, and experimental work focused on understanding cosmic ray interactions within the Standard Model of particle physics, and (ii) work on predictions and searches for physics beyond the Standard Model. Of course, both subjects are very closely related.

Cosmic ray interactions within the Standard Model

One of the key issues for doing particle physics with cosmic rays is that of knowing the primary cosmic ray flux, which serves as high-energy particle beam. Whereas we know the overall particle flux reasonably well, the results on elemental composition at energies greater than 10^{13} eV are subject to large systematic uncertainties [1, 2, 3, 4].

In the past the limited statistics and systematic uncertainties of the measurements were the main sources of uncertainty. Only recent cosmic ray detectors allow such a measurement accuracy and high statistics that now the uncertainties are dominated by our limited knowledge of modeling hadronic interactions. Prominent examples are the ongoing efforts of determining the elemental composition from high statistics data in the knee energy range (for example, KASCADE, EAS-TOP, GRAPES) and above 10^{18} eV (AGASA, HiRes, Auger), see [4]. In addition, there are several experiments designed to measure in the energy region of the transition from galactic to extragalactic cosmic rays (KASCADE-Grande, IceCube with IceTop, AMIGA & HEAT extensions of the southern Auger Observatory, TALE), which are expected to provide high quality data. The situation is similar for modern measurements of atmospheric muon and neutrino fluxes and muon charge ratio data.

To interpret the data of these experiments we have to understand the sources and the overall size

of the theoretical uncertainties of simulated reference showers, that are compared to data to derive the primary particle energy distribution and mass composition. In particular, estimating the size of the uncertainty of the theoretical predictions on air shower observables is currently one of the most important and unsolved problems[1].

Alternatively, cosmic ray data can be used learn more about particle interactions at high energy. For example, interaction models that allow an overall consistent description of different observables and different data sets are clearly favored and provide some clues of the general features of hadronic multiparticle production beyond the reach of colliders. Of particular importance is the proper description of different shower observables and their fluctuations on a shower-to-shower basis.

A much more direct method of studying the interaction characteristics is the selection of showers of almost mono-elemental composition to perform measurements with showers initiated by particles of known energy and mass. This approach is typically very difficult to implement as the criteria for selecting events are themselves depending on interaction models. External information coming from, for example, astrophysical models of the composition of cosmic rays in certain energy ranges [7, 8] or even angular correlations with potential sources [9] can be the key to the success of this method.

Reliability of the interpretation of air shower data

In the following we will concentrate on air shower simulations and only briefly comment on predictions of atmospheric secondary particle fluxes.

Sources of uncertainty of the predictions of air shower observables can mainly be related to (i) shortcomings and limitations of shower simulation techniques (for example, effects related to thin sampling of secondary particles), (ii) shortcomings in the simulation of the electromagnetic shower component, and (iii) uncertainties in the simulation of hadronic multiparticle production and resonance decay. In addition, the number of simulated showers and hence the statistical significance of the Monte Carlo data set, often limited by the available computing resources, is still an important issue, see Sec. 2.4.

It is generally assumed that electromagnetic interactions are well understood as we can calculate them reliably within perturbative QED. Current state-of-the-art simulation codes for electromagnetic showers such as EGS4 [26], EGSnrc [27], and FLUKA [28] are all based on leading-order QED predictions. Many predictions of the EGS and FLUKA packages have been verified in beam dump experiments at CERN and SLAC at energies below 1 TeV. Since most electromagnetic particles in a shower have energies in the MeV to GeV range, the uncertainty of the description of overall electromagnetic shower features, in particular the longitudinal profile, should be small. On the other hand, the particle densities at large lateral distance from the shower axis were never compared to accelerator data. Therefore, although we have no indication of serious shortcomings of current electromagnetic shower simulations, it would be worthwhile to check the size of next-to-leading order QED corrections at very high energy and also perform accelerator measurements at large distance to the shower core.

The main source of uncertainty of air shower predictions is currently the limited knowledge of hadronic multiparticle production at very high energy ($E > 10^{15}$ eV) and in the forward phase space region close to the direction of the incoming particle [34, 31]. Although QCD is the well-established theory of strong interactions, the bulk of the secondary particles produced in hadronic interactions can still not be predicted. Perturbative QCD calculations allow only the prediction of particle production in processes with large momentum transfer, which constitute just a small fraction of all interactions. Therefore we have to rely on measurements of particle production at accelerators and phenomenological models to extrapolate the measurements to the full energy and phase space ranges needed for air shower simulation. The range over which accelerator data have to be extrapolated is illustrated in Fig. 1. The energies accessible at accelerators are indicated by arrows. In addition the equivalent center-of-mass (CMS)

1. Taking advantage of the limited energy range of interactions of importance, remarkable progress has be made in estimating the uncertainty of neutrino flux predictions, see [5, 6].

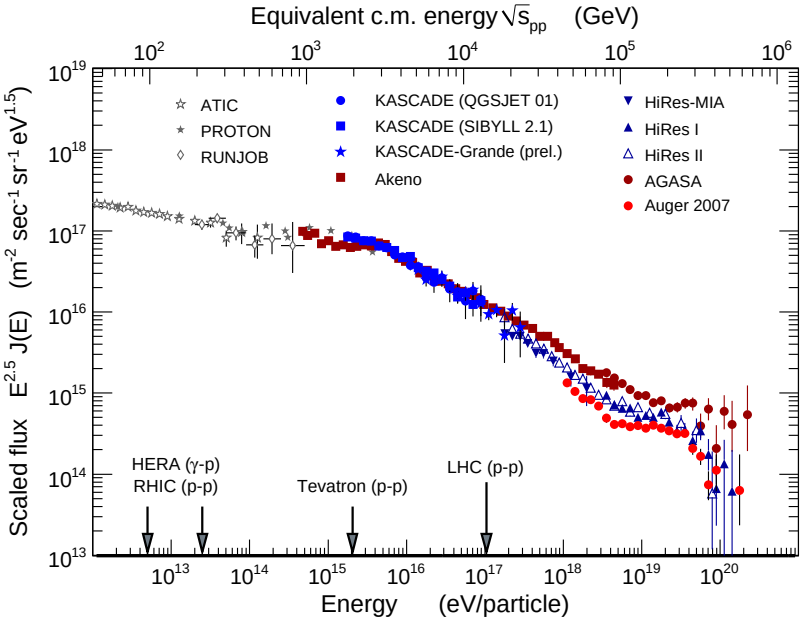

Fig. 1. Comparison of cosmic ray and accelerator energies. A representative set of flux measurements is shown to indicate the different features of the cosmic ray flux. The direct measurements on top of the atmosphere are from ATIC [10, 11], PROTON [12, 13], and RUNJOB [14]. The air shower measurements are KASCADE data (interpreted with two hadronic interaction models) [15], preliminary KASCADE-Grande results [16], and Akeno data [17, 18]. The measurements at high energy are represented by HiRes-MIA [19, 20], HiRes I and II [21, 22], AGASA [23, 24], and Auger [25].

energy for individual nucleon-nucleon collisions is shown for proton primaries.

Hadronic interaction models are typically divided into low- and high-energy models. Low-energy models describe hadronic interactions in terms of intermediate resonances (for example, the isobar model) and parametrizations of data. They are applicable in the energy range from the single particle production threshold up to several hundred GeV. Models that are frequently applied in simulations are FLUKA[2] [28], GHEISHA [35], UrQMD [36], and the more specialized code SOPHIA [37]. Low-energy models benefit from the existence of many data sets from fixed target measurements. Still the differences between the model predictions are significant and can lead to very different muon densities in air shower simulations [38, 39].

High-energy interaction models are typically very complex and make use of asymptotic expressions from Regge theory [40], Gribov's Reggeon calculus [41], and perturbative QCD. Central elements of these models are the production of QCD minijets and the formation of QCD color strings that fragment into hadrons. The currently used models are QGSJET 01 [42, 43] and II [44, 45], SIBYLL 2.1 [46, 47, 48], EPOS 1.6 [49, 50, 51] and DPMJET II [52] and III [53, 54]. The extrapolation of these models to very high energy depends on the internal structure of the model and the values of the tuned model parameters and is, in general, rather uncertain. Different extrapolations obtained within one model by varying the parameters can be found in [55, 56] and represent only a lower limit to the uncertainty of the predictions.

Consistency of air shower data description

The consistency of the description of different cosmic ray data sets is an indirect measure of the re-

2. FLUKA is a complete cascade simulation package that includes both low- and high-energy models.

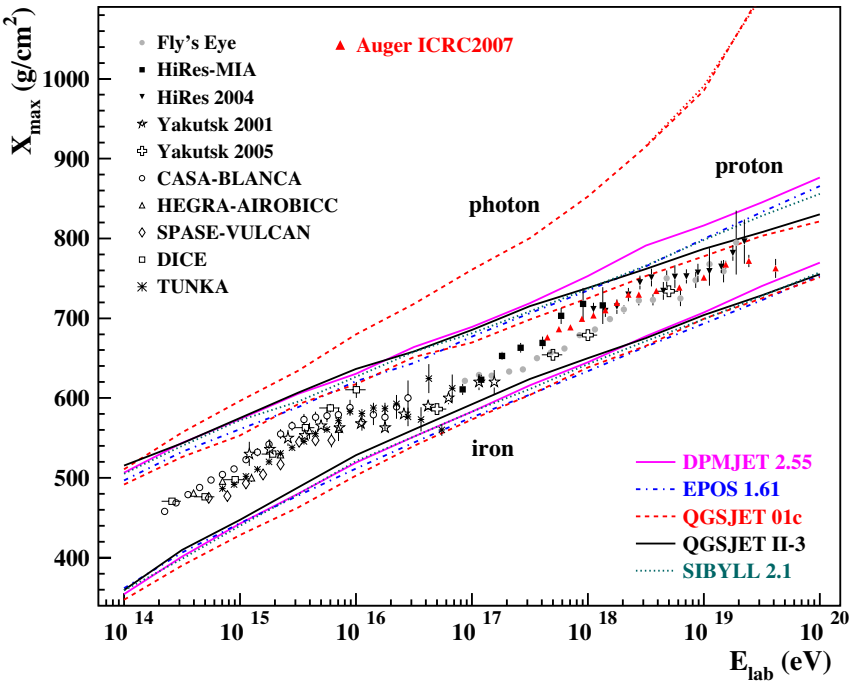

Fig. 2. Mean depth of shower maximum $X_{\max}$ [29]. Shown is a compilation of data together with predictions calculated with CORSIKA [30] and different interaction models. References to the data can be found in [31]. New results on $\langle X_{\max}\rangle$ have been presented at this meeting by the Auger [32] and HiRes [33] Collaborations.

liability of our current interpretation of air shower data.

There are several data sets that overlap in energy range and are taken with different detection methods that are either sensitive to the muonic and electromagnetic components in the shower at ground (particle detector arrays) or the longitudinal development of the shower profile (optical detectors). Of particular importance are the data of those detector installations that allow multi-component measurements and, hence, several independent composition analyses of the same data set.

In the following we discuss composition data sets with the emphasis on aspects related to the characteristics of hadronic interactions. The baseline for comparison will be QGSJET and SIBYLL: these models have been available for several years now and many groups have analyzed their data with them.

A compilation of measurements of the mean depth of shower maximum is shown in Fig. 2. All model predictions for proton and iron primaries bracket the data over the entire energy range. A change of composition is clearly visible between $10^{15.3}$ and 10^{17} eV. It is also worthwhile to notice that the prediction of the superposition model for the relation between the depth of shower maximum of a primary nucleus with mass number A and that of a proton-induced shower,

$$\langle X^A_{\max}(E)\rangle = \langle X^p_{\max}(E/A)\rangle, \qquad (1)$$

is approximately satisfied for all models.

The energy dependence of $\langle X_{\max}\rangle$ can be described by the elongation rate

$$D_{10} = \frac{d\langle X_{\max}\rangle}{d\lg E}.$$

The elongation rate of hadronic showers is approximately related to that of electromagnetic showers ($D^{\rm e}_{10} \approx 85$ g/cm^2) by

$$D^{\rm had}_{10} = D^{\rm e}_{10}(1 - B_n - B_\lambda), \qquad (2)$$

which is called the elongation rate theorem [57]. Here $B_n = \frac{d \ln n_{\rm tot}}{d \ln E}$ is the energy dependence of the multiplicity of secondary particles with high energy and $B_\lambda = -\frac{1}{X_0} \frac{d\lambda_{\rm int}}{d \ln E}$ characterizes the rise of the interaction cross section, with X_0 being the electromagnetic radiation length (for a detailed discussion, see [58]). If a model exhibits perfect scaling, i.e. the secondary particle distributions are only functions of the variable $x = E_{\rm sec}/E_{\rm prim}$, and has a slowly rising cross section, its elongation rate will be close to that of electromagnetic showers.

The correlation between the influence of scaling violations and of the rise of the cross section on the elongation rate makes the interpretation of $\langle X_{\rm max} \rangle$ in terms of the characteristics of hadronic interactions difficult. For example, SIBYLL exhibits a rapidly rising cross section and only mild scaling violation of the secondary particle distributions, whereas QGSJET 01 is characterized by a cross section that rises moderately fast with energy and predicts much larger scaling violations.

Due to the limited knowledge of simulating hadronic interactions, it is possible to have the highest energy $\langle X_{\rm max} \rangle$ points corresponding to a pure proton composition if interpreted with a modified version of SIBYLL or QGSJET. On the other hand, using a model with nearly perfect scaling and slowly rising cross section, the data point around 10^{19} eV could be interpreted equally well as a pure iron composition.

There are indeed indications that models with smaller scaling violations are favored on the basis of other data sets, however, the pure iron interpretation seems to be unlikely if the highest energy point of the new Auger data [32] is not just a downward fluctuation. More data at the highest energies will help to distinguish between these scenarios. Furthermore, a measurement of the $X_{\rm max}$ fluctuations will be decisive in this case. Whereas it is difficult to distinguish a pure proton composition from a mixed one of intermediate elements, a pure iron composition will have such small fluctuations that the width of the $X_{\rm max}$ distribution can be used as unique signature.

A compilation of mainly surface detector based measurements of the elemental composition at the highest energies is shown in Fig. 3. The composition sensitivity of surface detector observables stems from the fact that the muon number N_μ scales with mass number A approximately as

$$N_\mu^{(\rm A)} = A \left(\frac{E}{A E_{\rm dec}} \right)^\alpha = A^{1-\alpha} N_\mu^{(1)}, \quad (3)$$

with

$$\alpha = \frac{\ln(n_{\rm ch})}{\ln(n_{\rm tot})} \approx 0.9. \quad (4)$$

Here $E_{\rm dec}$ is a typical energy scale for the decay of muons and $n_{\rm tot}$ and $n_{\rm ch}$ are the total and charged particle multiplicities, respectively (for a detailed discussion, see [66]).

There seems to be good general agreement between the $X_{\rm max}$ composition trend to lighter elements with increasing energy and the surface detector data of Fig. 3. When comparing the different results it is important to keep in mind that the surface data were analyzed with different versions of QGSJET and SIBYLL. Whereas QGSJET 98 predictions are very similar to those of QGSJET 01, the results obtained with SIBYLL 2.1 are different from those based on SIBYLL 1.6. Therefore Figs. 2 and 3 can only be compared on a qualitative level.

Indeed, more direct comparisons using the same hadronic interaction models reveal a systematic inconsistency between composition results based on surface detector data and that based on the measurement of the mean depth of shower maximum [68]. Analysis of the surface detector data lead to a heavier primary composition than one would expect from $\langle X_{\rm max} \rangle$ data. This is most clearly seen in experiments that measure both $X_{\rm max}$ and the number of muons or related quantities. There are two such data sets available. The prototype experiment HiRes-MIA [69] studied showers in the energy range from 10^{17} to $10^{18.5}$ eV. The measured muon densities at 600 m from the core could only be interpreted as iron-dominated composition, but the mean $X_{\rm max}$ indicated a transition to a proton-dominated composition [20].

With the Auger data presented at this conference [67], this discrepancy is impressively confirmed with several independent analyses at about 10^{19} eV. Using universality features of very high energy showers $E > 10^{18}$ eV, one can relate the electromagnetic shower size at a lateral distance of 1000 m to the shower energy and the depth of

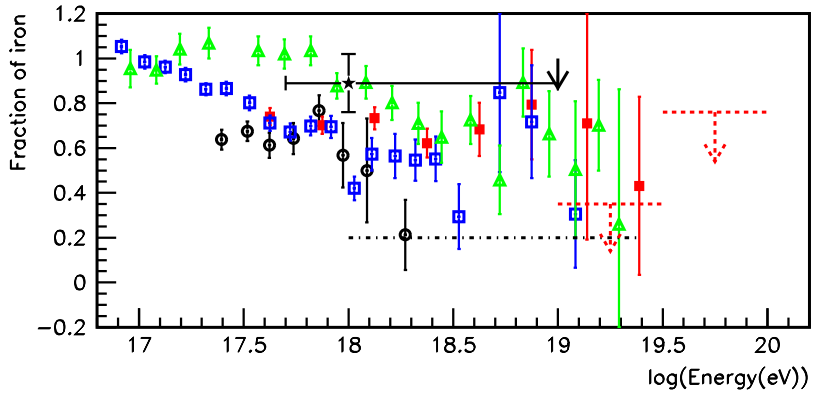

Fig. 3. Iron fraction if data are interpreted as a superposition of proton and iron showers [59]. The data are from Fly's Eye (△), AGASA A100 (■), AGASA A1 (□) using SIBYLL 1.6 ([60] and references therein) and Haverah Park [61], using QGSJET 98 (○). The mean composition determined in [62] with the corresponding error for the Volcano Ranch energy range using QGSJET 98 is shown as (⋆). The solid line arrow indicates the result using rise time measurements from Haverah Park [63]. The dashed arrow lines represents upper limits obtained by the AGASA Collaboration with QGSJET 98 [64] and the dot dashed horizontal line is the result of the HiRes analysis [65].

shower maximum [70, 71, 72]. The employed universality features are the same for showers simulated with the interaction models QGSJET II and SIBYLl 2.1. Considering showers at different angles and employing the independently measured depth of shower maximum, the observed muon signal can be set in relation to the predicted muon signal as shown in Fig. 4. Adopting the nominal energy scale of the Auger fluorescence detectors, the number of muons at 1000 m from the core is found to be twice as large as predicted by simulations with proton showers. This number should be compared to that of iron-induced showers for which one expects a muon number increased by the factor 1.38 (QGSJET II) or 1.27 (SIBYLL 2.1). Increasing the energy scale by 30% as the constant intensity cut analysis of the data suggests and assuming a iron dominated composition seems to bring the data into agreement with the model predictions. This is, however, not really the case since the $\langle X_{\rm max}\rangle$ data is at variance with the iron composition hypothesis at 10^{19} eV.

We are forced to interpret the discrepancy between the Auger data and the model predictions as a serious shortcoming of current current interaction models. The most straightforward solution to this puzzle would be an increase of the predicted muon number of the models by about 30%. On the other hand, the muon number is a rather robust quantity and changing only the characteristics of the first few interactions of the hadrons during the shower startup phase seems not enough to increase the muon number significantly [73]. For example, one would have to increase the secondary particle multiplicity of the first interaction by a factor of 10 to increase the overall muon number by 25%.

Another way of decreasing the discrepancy between data and models is the modification of the scaling behavior (for example, see study with QGSJET 01 in [68]). A reduction of the scaling violation and the cross section of a model does not change very much the predicted muon number but strongly influences the depth of shower maximum. This way it is possible to describe the measured $\langle X_{\rm max}\rangle$ with iron-like showers. Interestingly, a recent study of the inclusive muon fluxes at high energy also indicates that nearly perfect scaling of the distributions of energetic secondary particles in the primary energy range from 10^{12} to 10^{17} eV is favored [74].

Finally it should be mentioned that indications for an excess of muons have been observed also in other experiments at various energies, although in a much less direct way. Examples are the observations of very high multiplicity muon bundles with LEP detectors [75, 76, 77] and the downward

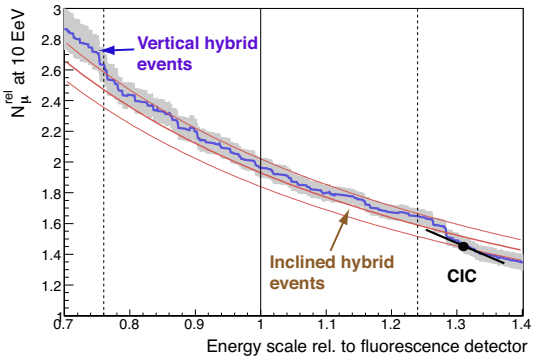

Fig. 4. Muon number relative to the prediction of QGSJET II for proton primaries in dependence on the energy scale of the fluorescence detector [67]. Shown are the results of the constant intensity cut method (CIC) and the analysis of vertical hybrid events ($\theta < 60^\circ$) and inclined hybrid events ($\theta > 60^\circ$).

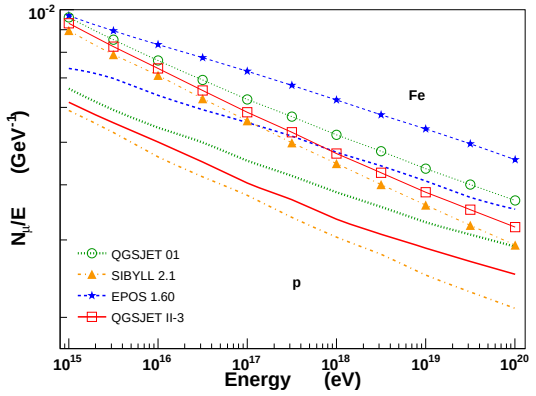

Fig. 5. Muon number of proton- and iron-induced air showers simulated with EPOS 1.6, QGSJET II and SIBYLL [51]. For clarity, the muon number is divided by the shower energy.

going muon flux measured with AMANDA [78]. This muon excess cannot be explained with charm production in air showers, which currently is neglected in most simulations [79].

The knee energy range is very well suited for testing the consistency between data and hadronic interaction models. If the entire energy range of transition from the light mixed composition below 10^{15} eV to the presumably iron dominated composition at higher energy is covered by one detector, a model can be tested for both light and heavy primaries. The classic composition analysis of the KASCADE Collab. has shown that none of the current interaction models gives a consistent data description [15, 80]. SIBYLL 2.1 and, to a lesser extent, also QGSJET II seem to predict too few muons already at energies just above $10^{15.5}$ eV. The independent data set of the GRAPES 3 detector installation [81] will be very important to confirm these discrepancies. The GRAPES data presented at this meeting [82, 83] are very promising, but a complete unfolding of several elemental groups as done by the KASCADE Collab. has not yet been attempted. First results indicate that an analysis with QGSJET II and SIBYLL 2.1 leads to very similar primary fluxes that are in reasonable agreement with the extrapolation of direct measurements [83].

Alternative interaction models

The recently developed interaction model EPOS 1.6 [49, 50, 51] is the successor to the neXus model [84]. Compared to models like SIBYLL and QGSJET, the philosophy of this model is different and motivated by the rich and very complex data sets from the RHIC collider. In favor of obtaining a very good description of existing accelerator and collider data, some internal distributions had to be parametrized in EPOS. In particular, in contrast to all other models, it is assumed that the fragmentation of strings changes in dependence on the overall energy density in the phase space region of the string [49]. These modified string fragmentation parameters can be considered as an effective implementation of parton-parton fusion in phase space regions of very high parton density, a phenomenon often referred to as saturation [85]. The non-universality of the fragmentation parameters comes along with the introduction of a number of additional parameters, which make the EPOS model more flexible in describing RHIC measurements. A comparison with QGSJET and SIBYLL shows that EPOS-simulated interactions are characterized by different leading particle distributions at high energy (strong scaling violation for leading nucleons) and also a considerably higher multiplicity of produced baryon-antibaryon pairs. The higher antibaryon production seems to be supported by several data sets [50, 51], though the data are not fully conclusive.

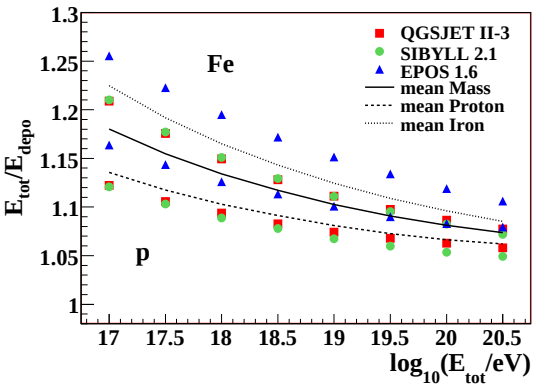

Fig. 6. Correction factor needed for scaling up the measured calorimetric energy of an air shower to obtain the total primary energy [86].

One of the most interesting features of the EPOS model with respect to air shower physics is the prediction of a much higher number of muons in hadronic showers, see Fig. 5. There are basically two processes linked to this enhanced muon production that have been identified so far.

- The larger multiplicity of secondary baryon-antibaryon pairs enhances the hadronic component of the shower [50]. Baryons cannot decay into electromagnetic particles as is the case for neutral pions. Due to baryon number conservation, they will always be present in the cascade and can produce many secondary pions when cascading down to very low energy, an effect that has been pointed out already in [87].

- The projectile fragmentation can lead to a significant enhancement of muons, if – averaged over all interactions in the shower – there are fewer leading neutral pions produced. This aspect of the leading particle flavor distribution is discussed in detail in [88].

Both effects are based on conventional physics that is already present at low energy and can, therefore, be tested with new collider data.

The higher number of muons predicted by EPOS has several important consequences. If EPOS is adopted for generating reference showers, the interpretation of muon number based composition measurements will be significantly different. Fig. 5 shows that, at 10^{18} eV, a data set previously interpreted as corresponding to an iron dominated composition could now be considered as proton dominated! Furthermore the higher number of muons modifies the correction that has to be applied to fluorescence telescope measurements to obtain the total shower energy (often called missing energy correction). This is shown in Fig. 6.

A very good test of these drastic changes of the composition interpretation of existing data can be made by analyzing the KASCADE electron-muon correlation data in the knee energy region. Even at this energy the muon numbers predicted with EPOS are much higher than that of the other models. A first test done by the KASCADE Collab. shows that the EPOS model predicts too high a muon number for a given number of electrons and the flux derived with it is too high if compared to direct measurements [89]. It will be very important to find out whether this disagreement effectively limits the muon number in showers in the knee energy region to that of models like QGSJET II or whether some other modifications of EPOS – for example, a change of the electron number – can lead to a better agreement with KASCADE data.

Another, alternative approach to simulating interactions at ultra-high energy is that based on string fusion. The key assumption here is that the QCD color strings formed by the interaction of partons in the projectile and target particles are expected to fragment independently only up to a certain energy density in phase space. If strings come very close to each other in phase space they can fuse to a new string with different properties. The particles produced in the fragmentation of fused strings have higher transverse momenta, the total multiplicity is decreased (if compared to a scenario without string fusion), the fraction of heavy particles including kaons and baryon-antibaryon pairs is increased, and the leading particle spectrum changes [90, 91, 92, 93, 94, 95, 96, 97]. A phase space transition in hadron production is predicted in a situation with high string density, in which not only two strings fuse but multiple mergers finally lead to percolation. A number of observations made in heavy ion collisions at RHIC are successfully described within this model [98, 99]

The impact of string fusion and percolation on air shower predictions has been considered in dif-

ferent publications, partially by using simple analytical expressions to describe the energy dependence of the depth of shower maximum and muon number [100, 101] and also by performing numerical simulations [102, 103, 104, 105]. There are different effects that are potentially important. For example, the strong reduction of the rise of the multiplicity of secondary particles with increasing energy can lead to a larger elongation rate than predicted by current models [100]. Depending on the parameters, this reduction could explain, at least partially, the large elongation rate measured with the HiRes-MIA setup [20], changing the interpretation of the data in terms of a necessary change of mass composition. Another important effect of string percolation is the modification of the leading particle spectra and, hence, the elasticity[3] of the interactions [101]. In addition, any modification of the flavor of the leading particle is of great importance for the shower characteristics [104].

Although these effects are very promising means of explaining many structures of the $\langle X_{\rm max}\rangle$ data without the need of a changing cosmic ray composition, simulations show that there is a gradual transition from one scenario to another before these effects are fully efficient and modify the shower predictions. Moreover, it can be argued that string fusion and percolation might explain an elongation rate as large as $\sim 75\,\mathrm{g/cm^2}$, but so far no scenario is known that might reduce the elongation rate at higher energy again to the observed $\sim 50\,\mathrm{g/cm^2}$ per decade in energy.

For completeness and to illustrate the full range of uncertainty, we contrast the string fusion scenario predicting a large elongation rate and slow increase of the muon number with a model that predicts just the opposite, even though it has not been presented at this meeting. If the perturbative QCD predictions for parton densities are extrapolated to small momentum fractions of the partons within the Balitsky-Fadin-Kuraev-Lipatov approximation [118], the density of gluons increases to such an extend that one can speak of black disk scattering in non-peripheral collisions [119]. In this case the the "classic" particle remnants will fully disintegrate and all partons will acquire a transverse momentum in the collision that is larger than a typical saturation scale [120]. The elasticity of the interactions decreases drastically, leading to a very small elongation rate in air showers (below $\sim 45\,\mathrm{g/cm^2}$) [120]. In a more realistic simulation the effect will be smaller since many collisions are peripheral and will not yet have reached the black disk limit.

The string fusion and percolation model and the black disk limit model provide different ways of describing new phenomena that are expected for very large parton densities, often referred to as *parton saturation*. The models EPOS 1.6, QGSJET II, and SIBYLL 2.1 have ideas and parametrizations implemented that address the same high parton density phenomena in again different ways and different levels of sophistication. It is mainly the lack of a theory and data on parton saturation phenomena that leads to the observed uncertainty of the model predictions.

Cross section measurements

The proton-air cross section determines not only the depth of the first interaction in an air shower, it also influences how fast a shower develops. Several updated and new attempts to measure this cross section have been presented at this meeting [121, 122, 123]. The key observation is the good correlation between the overall shower profile and the depth of the first interaction. This correlation is particularly good for the depth of shower maximum and somewhat worse for ground array observables that effectively are related to the shower age (for a recent discussion, see [106]).

There has been some confusion regarding the part of the proton-air cross section that is measured in cosmic ray experiments. It is clear that, even under ideal conditions, only the particle production cross section can be measured. Any interaction without production of new particles will not influence the development of an air shower. In proton-nucleus collisions, the total cross section can be written as

$$\begin{aligned}\sigma_{\rm tot} &= \sigma_{\rm ela} + \sigma_{\rm inel} \\ &= \sigma_{\rm ela} + \sigma_{\rm q-ela} + \sigma_{\rm prod}, \end{aligned} \quad (5)$$

where $\sigma_{\rm ela}$ and $\sigma_{\rm inel}$ denote the elastic and inelastic cross sections, respectively. The inelastic cross section is the sum of the cross section for

3. Elasticity is defined here as the energy fraction carried by the most energetic secondary hadron that interacts again deeper in the atmosphere.

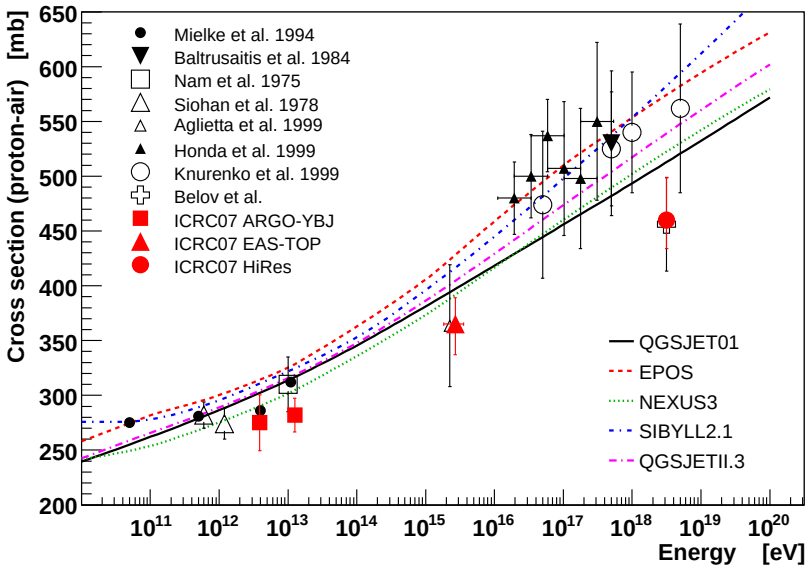

Fig. 7. Compilation of proton-air particle production cross sections [106]. Shown are data [107, 108, 109, 110, 111, 112, 113, 114, 115, 116, 117] and model predictions. Data labeled with "ICRC07" have been presented at this meeting.

quasi-elastic scattering ($\sigma_{\mathrm{q-ela}}$) and that of particle production σ_{prod}. Quasi-elastic processes are interactions, in which the incoming proton is elastically scattered on at least one of the nucleons of the target nucleus, leading to a nucleus breakup without production of "new" particles such as pions or kaons. The quasi-elastic cross section amounts to about $\sim$ 10 % of the inelastic cross section. In Monte Carlo simulations of hadron-air interactions, only the production cross section is used[4] and consequently, it is this cross section that is derived in the analysis of data from cosmic ray experiments.

Fig. 7 shows a compilation of proton-air cross section measurements [106]. The low-energy data are obtained from analyses of the unaccompanied hadron flux in the atmosphere and high energy data are from air shower observations.

The measurement of the proton-air cross section is difficult. First of all, there are not only protons in the cosmic ray beam. Any analysis needs to employ cuts that select proton-induced showers. Secondly, the correlation function describing the relation between the measured air shower observables and the depth of the first interaction point has to be taken from simulations and depends itself on the proton-air cross section and other unknown variables. Both sources of uncertainty have been discussed at this conference [124, 121, 122, 123].

Currently there is no solution known for removing a possible bias due to the unknown and most likely mixed primary cosmic ray composition. Simulations with other primaries such as helium or gamma-rays are performed and the systematic uncertainty estimated [122, 123, 121]. This procedure is expected to give good results if the composition is indeed proton dominated but will fail otherwise.

An improved cross section analysis method has been put forward that accounts for the cross section dependence of the correlation between the first interaction point and the depth of shower maximum [124]. By assuming that the cross section is known at 10^{15} eV, equivalent to Tevatron c.m.s. energy, one can interpolate (logarithmically in energy from 10^{15} eV to the air shower energy) the

4. In case of primary nuclei and their fragments, the inelastic cross section is simulated.

correction factor needed to bring the hadronic interaction model cross section in agreement with the measured one. This rescaled cross section is then used in the simulations for the data analysis in either an iterative procedure or by parametrizing the dependence of the correlation function on the high energy cross section. Further assumptions are that the same correction factor can be applied to pion- and kaon-air cross sections. Monte Carlo studies show that the model dependence can be greatly reduced even though the application of a scaling factor to the cross section leads to a "modified" interaction model, in which particle production and cross section are no longer self-consistent.

Keeping the uncertainties of the cross section measurements in mind, it is still worth noting that all new measurements fall below the current model predictions, see Fig. 7. It is clear that air shower measurements are not sensitive to the total particle production cross section. For example, there are final state configurations such as target diffraction dissociation that are indistinguishable from elastic interactions. Still, the difference between data and model predictions is not related to this "invisible" part of the cross section since the measured cross section is corrected back to the full particle production cross section in all analyses. The discrepancy is particularly interesting for the data points up to $\sim 10^{15}$ eV. The proton-proton cross section is well-known in this energy range and, hence, the predicted proton-air cross section can be used to test Glauber's multiple scattering theory [127]. The data indicate larger than previously assumed inelastic screening corrections [128], which reduce the proton-air cross section for a given proton-proton cross section.

Accelerator data on multiparticle production

Accelerator data are needed for tuning interaction models and also allow us to test certain aspects of these models. The longitudinal profile of air showers is mainly governed by the characteristics of high-energy interactions. Particle densities at large lateral distances depend on both high- and low-energy interactions [38, 39]. Hadronic interactions at low energy are also of direct relevance to muon and neutrino flux calculations [129, 5, 130] and background suppression of imaging atmospheric gamma-ray telescopes [131, 132]

Low-energy interactions can be measured in fixed target experiments, which also allow good coverage of the forward particle production hemisphere. Although in fixed target setups the target material can be chosen almost freely, there is a lack of dedicated measurements of hadronic interactions with light nuclei. Nitrogen and oxygen can only be used in cryogenic targets increasing the costs of the experiments. Some data in the relevant mass range exist for carbon and beryllium nuclei [133, 134].

The situation has improved recently with the publication of HARP data on p-C and π-C interactions at 12 GeV [125, 126] and NA49 data on p-C interactions at 158 GeV [135, 136]. Moreover, the HARP Collab. performed also measurements with liquid N_2 and O_2 targets, which were presented at this meeting [125]. Both the HARP [137] and the NA49 [138] detectors are providing very good particle identification and momentum reconstruction in the forward direction.

In Fig. 8 the inclusive cross section for π^+ production on carbon at 12 GeV is shown. The data are compared with the predictions of the models DPMJET III, GHEISHA, and UrQMD. None of the interaction models gives a fully consistent description of the data. The situation is similar for the production of negative pions. A comparison of the NA49 data set with different models can be found in [139].

There are two groups that plan to take further data suited for tuning cosmic ray interaction models. The NA61 experiment is the successor to NA49 at the CERN SPS. Its detector is based on the setup of NA49 with additions to improve particle identification at larger angles. The NA61 Collab. took first physics data with a 30 GeV proton beam on carbon target in 2007. One of the aims of the NA61 experiment [140] is the measurement of secondary particle yields suited as reference spectra for the T2K neutrino oscillation experiment [141]. The experiment MIPP (Main Injector Particle Production experiment) at Fermilab aims at the measurement of secondary particle spectra for a beam of $\pi^{\pm}$, $K^{\pm}$, and $p^{\pm}$ in the energy range from 5 to 90 GeV. First physics data were taken in 2005 and 2006 [142]. MIPP has

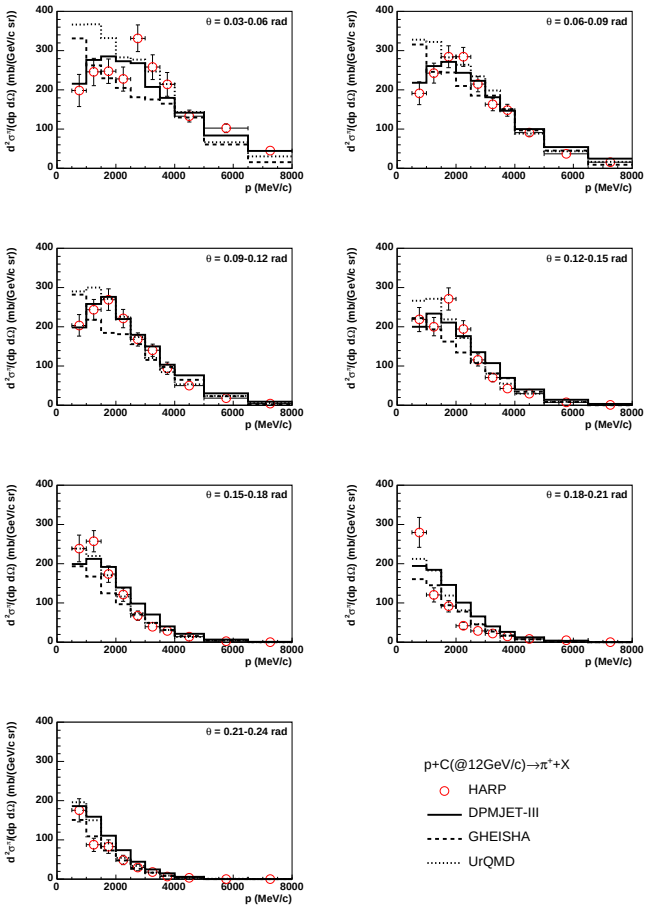

Fig. 8. HARP data of positive pion production on a carbon target at 12 GeV beam energy [125, 126]. The error bars indicate systematic and statistical errors added in quadrature. The data are compared with model predictions.

nearly full acceptance for charged particles. Currently the detector is upgraded with a faster DAQ to allow high-statistics measurements.

The LHC will be the new high energy frontier. The dedicated forward experiment LHCf [143, 144, 145] will take data in the early low-luminosity phase of the collider and allow the measurement of the distribution of π^0 and neutrons. The detectors are installed to both sides of the interaction point of the ATLAS detector. The TOTEM setup will allow the measurement of the total and elastic cross sections and the slope of the forward scattering amplitude [146]. The ATLAS and CMS Collabs. have begun to prepare their detectors for forward physics studies also suited for better understanding cosmic ray interactions. For example, the CMS detector will be operated together with the CASTOR [147] and TOTEM [146] detectors and a zero-degree calorimeter for neutral particles, see [148].

Simulation techniques and tools

Simulations fall into different categories, those aimed at calculating mean quantities and those focused on the simulation of individual showers with their physics fluctuations. For example, for the calculation of inclusive secondary particle fluxes, it is sufficient to know the mean value of the observables with high precision. On the other hand, in

many air shower experiments, the simulation of individual showers with their fluctuations is of interest. One of the key problems here is the application of thin sampling [149]. Only a representative subset of particles is explicitly followed in a shower and, by assignment of statistical weights, the overall shower features are reconstructed. This procedure leads to an increase of non-statistical fluctuations on top of the necessary increase of the statistical fluctuations due to the smaller number of particles.

If only mean quantities are of interest, it is very efficient to simulate many showers with rather crude thinning. This method can be extended to individual showers by simulating the high-energy part of the shower only once and without thinning and then apply thinning to many realizations of the low-energy part of the same shower [150, 151]. The procedure makes use to the fact that most of the shower-to-shower fluctuations are the result of fluctuations of the high-energy interactions in the early shower development stages.

Hybrid simulation codes apply the same idea but replace the explicit Monte Carlo simulation of low-energy interactions either by a library of showers [58] or a system of cascade equations that is solved numerically for the given initial conditions [152, 153].

One of the difficult tasks is the comparison of the predictions of hybrid simulation programs with that of classic Monte Carlo codes. The simulation of many showers of very high energy with Monte Carlo is not feasible in this case. To make sure that the uncertainty of such a comparison is not dominated by the small statistics of the showers generated with the standard Monte Carlo simulation code, one can simply concentrate on a set of selected high energy showers. For these showers the high energy interactions are generated without thinning and used later in both the Monte Carlo and the hybrid simulation simulations [154]. This procedure minimizes the influence of physics fluctuations on the model comparison.

Finally it should be mentioned that the efficiency of very detailed simulations of ultra-high energy showers is improved considerably by simulating subshowers on individual nodes of parallel computing clusters [155]. By filling the longitudinal and lateral particle profiles in a database, the simulated showers can be used later to obtain high accuracy simulations even at the highest energies [156].

Simulation of radio signals from showers

The status and recent advances in the field of radio detection of cosmic rays and neutrinos will not be covered here. This subject is reviewed in a highlight talk and the corresponding proceedings contribution [157] and the part of relevance to neutrino physics is summarized in [6].

Searches for phenomena beyond the Standard Model

Cosmic ray detectors are often very well suited to perform searches for exotic particles such as monopoles or for annihilation products of dark matter particles. In this sense, the contributions to the sessions HE 3.3 - 3.5 covered only some particular aspects of the wide and very complex field of particle searches. The interested reader is referred to dedicated conferences for a comprehensive review of the status of the field.

Dark Matter

Detecting secondary particles produced in the annihilation or decay of dark matter particles can give clues of the mass, type and distribution of the unknown dark matter particles. Often the neutralino, the lightest supersymmetric particle, is theoretically favored as candidate for dark matter, but also many other hypotheses have been put forward [158]. Assuming that the dark matter particles can annihilate (or decay) to gamma-rays and particle-antiparticle pairs, one can search for these secondary particle fluxes. Promising secondary particle channels are positrons, antiprotons, antideuterons (low background fluxes), gamma-rays, and neutrinos (particles point back to the source).

General limits on the annihilation rate of dark matter particles can be obtained over a wide range of particle masses from the comparison of the expected secondary fluxes with measured diffuse neutrino and gamma-ray fluxes [159, 160, 161, 162, 163].

To substantially improve these general limits, theoretical assumptions and model predictions are needed, in particular, on

- the dark matter distribution, including its clumpiness [164, 165, 166],
- the type and mass of the particle, and
- the propagation of secondary particles to Earth (if charged) [167, 168, 169]

For example, if the dark matter distribution is clumpy, the annihilation rate in the clumps can be much higher that expected for a smooth distribution [170, 164]. In general, the sensitivity of a search can be increased by looking at objects with a very high dark matter density [171]. Results on such searches have been reported by AMANDA (neutrinos from Sun and Earth) [172], H.E.S.S. (gamma-rays from the Sagittarius dwarf galaxy) [173], MAGIC (gamma-rays from dark matter spikes around intermediate black holes and from the Draco galaxy) [174, 175], and AMS01 (diffuse positron flux) [176].

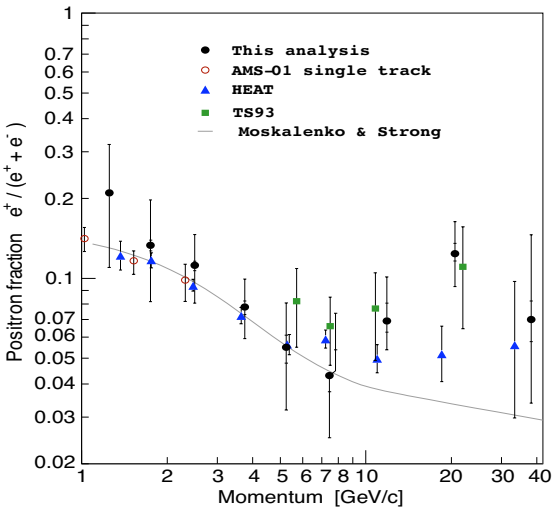

Fig. 9. Positron fraction in the total electron and positron flux measured at the top of the atmosphere. Shown are the results of the AMS01 analyses [177, 176], the early TS93 results [178], and the combined $e^{\pm}$ and $\bar{p}$ data from HEAT [179]. The curve shows the expectation for a model without an annihilation source for positrons [180].

The new analysis of AMS01 data [176, 177] is particularly interesting as it supports initial indications of an excess of the high energy positron flux at the top of the atmosphere that was found in TS93 and HEAT data [178, 179]. The standard positron identification with AMS01 was limited to energies below 3 GeV due to the large background from protons. Using positrons that emit a bremsstrahlung photon that converts to a e^+e^- pair, the measurement of the positron flux can be extended to 50 GeV. Fig. 9 shows the ratio of the positron flux to the total electron and positron flux in the energy range from 1 to 50 GeV. Data are compared with a prediction based on secondary positions without dark matter contributions.

Finally it should be mentioned that there is an ongoing debate whether it is possible to interpret EGRET gamma-ray data and measured antiproton fluxes consistently with an annihilation signal from ~ 70 GeV neutralinos [181]. Conventional cosmic ray propagation models predict too high a $\bar{p}$ flux at Earth for this scenario [182]. In a model scenario with dark matter annihilation in small scale clumps, this contradiction can be resolved due to magnetic field irregularities and small scale confinement of cosmic rays [167].

Direct searches for exotic particles

The searches for exotic particles discussed at the meeting cover a wide range from tachyons [183] over magnetic [184, 185, 186, 187] monopoles to Q-balls and strangelets [185, 188]. In the following we will consider only the results on magnetic monopoles.

Magnetic monopoles were first introduced by Dirac on the basis of topological arguments [189] and later found in the particle spectrum of Grand Unified Theories (GUT) [190, 191]. Their charge is an integer multiple of $e/2\alpha_{\rm em}$, where e is the electromagnetic charge and $\alpha_{\rm em}$ is the fine structure constant, and their mass is of the order of $\Lambda/\alpha_{\rm em}$, with Λ being the GUT scale.

Depending on the detection method, searches focus on sub-relativistic or relativistic monopoles ($\beta \geq 0.8$). Relativistic monopoles can be detected by Cherenkov light emission in dense media. The expected signal is about 8300 stronger than that of a electrically charged particle. Slow-moving, supermassive monopoles can be

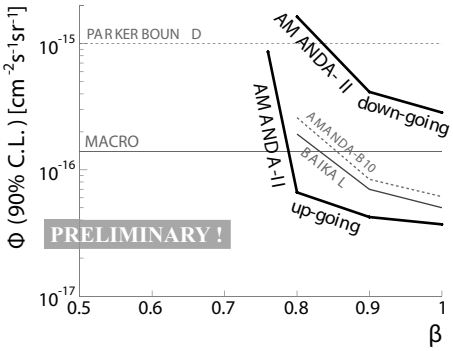

Fig. 10. Flux limits on relativistic monopoles. AMANDA II data [186] are compared with those of BAIKAL [192] and MACRO [193].

detected through the large number of leptons they produce along their path. These leptons are secondary particles of, for example, catalyzed nucleon decay reactions [194, 184].

Fig. 10 shows the current limits on the flux of relativistic monopoles. AMANDA II data presented at this meeting [186] are compared with the results from MACRO [193] and BAIKAL [192]. These limits can be improved considerably with data from the IceCube detector [195].

Forthcoming experiments

Much higher sensitivity to secondary particle fluxes from the annihilation of dark matter particles or to direct detection of exotic particles will be obtained with the forthcoming multipurpose instruments AMS02 [196, 197], GLAST [198, 199], and IceCube [200, 195]. Projects in the design phase are the General Antiparticle Spectrometer (GAPS) [201], which is planned to be flown in multiple long duration balloon flights, and the CALorimetric Electron Telescope (CALET) [202], which is proposed to be flown on the International Space Station.

Acknowledgments

It is a pleasure to thank the organizers for the very fruitful and stimulating conference. The author is very grateful to his colleagues from the Pierre Auger, KASCADE-Grande, and LOPES Collaborations for many helpful discussions.

References

[1] S. P. Swordy et al., Astropart. Phys. 18 (2002) 129.
[2] A. Haungs, H. Rebel, and M. Roth, Rept. Prog. Phys. 66 (2003) 1145.
[3] J.R. Hoerandel, Astropart. Phys. 19 (2003) 193.
[4] M. Teshima, Proceedings of the 30th ICRC, Mérida, México, 2007, Vol 6, p. 329.
[5] G.D. Barr et al, Phys. Rev. D 74 (2006) 094009.
[6] T.K. Gaisser, Proceedings of the 30th ICRC, Mérida, México, 2007, Vol. 6, p. 341.
[7] V.S. Berezinsky, S.I. Grigorieva, and B.I. Hnatyk, Astropart. Phys. 21 (2004) 617.
[8] V. Berezinsky, Proceedings of the 30th ICRC. Mérida, México, 2007, Vol. 6, p. 21.
[9] J. Abraham et al., (Pierre Auger Collaboration), Science 318 (2007) 939; J. Abraham et al., *Correlation of the highest energy cosmic rays with nearby extragalactic objects*, arXiv:0711.2256[astro-ph].
[10] H.S. Ahn et al., (ATIC-2 Collaboration), Prepared for the 28th ICRC, Tsukuba, Japan, 2003, p. 1853.
[11] J. Wefel, Private communication, 2006.
[12] N.L. Grigorov et al., Yad. Fiz. 11 (1970) 1058.
[13] N.L. Grigorov et al. Proceedings of the 12th ICRC, Hobart, 1971, Vol. 2, p. 206.
[14] V.A. Derbina et al. (RUNJOB Collaboration), Astrophys. J. 628 (2005) L41.
[15] T. Antoni et al. (KASCADE Collaboration), Astropart. Phys. 24 (2005) 1.
[16] A. Haungs et al. (KASCADE-Grande Collaboration), to appear in Proc. of XIV ISVHECRI, Weihai, China, 2006.
[17] M. Nagano et al., J. Phys. G 10 (1984) 1295.
[18] M. Nagano et al., J. Phys. G 18 (1992) 423.
[19] T. Abu-Zayyad et al. (HiRes-MIA Collaboration), Astrophys. J. 557 (2001) 686.
[20] T. Abu-Zayyad et al. (HiRes-MIA Collaboration), Phys. Rev. Lett. 84 (2000) 4276.
[21] P. Sokolsky (HiRes Collaboration), Proceedings of the 30th ICRC. Mérida, México, 2007, Vol 4, p. 473.
[22] R. Abbasi et al. (HiRes Collaboration), Phys. Rev. Lett. 100 (2008) 101101, arXiv:0703099[astro-ph].

[23] M. Takeda et al. (AGASA Collaboration), Astropart. Phys. 19 (2003) 447, arXiv:0209422[astro-ph].
[24] M. Takeda et al. (AGASA Collaboration), Prepared for ICRC, Tsukuba, Japan, 2003, p. 381.
[25] M. Roth (Auger Collaboration), Proceedings of the 30th ICRC, Mérida, México, 2007, Vol. 4, p. 327.
[26] W. Nelson et al., Stanford Linear Accelerator Center (1985) SLAC-265.
[27] http://www.irs.inms.nrc.ca/EGSnrc/.
[28] F. Ballarini et al., J. Phys. Conf. Ser. 41 (2006) 151.
[29] D. Heck, private communication, 2007.
[30] D. Heck et al., Wissenschaftliche Berichte FZKA 6019, Forschungszentrum Karlsruhe, 1998.
[31] J. Knapp et al., Astropart. Phys. 19 (2003) 77, astro-ph/0206414.
[32] M. Unger (Auger Collaboration), Proceedings of the 30th ICRC, Mérida, México, 2007, Vol. 4, p. 373.
[33] Y. Fedorova et al. (HiRes Collaboration), Proceedings of the 30th ICRC, Mérida, México, 2007, Vol. 4, p. 463.
[34] J. Knapp, D. Heck, and G. Schatz, in Wissenschaftliche Berichte FZKA 5828, Forschungszentrum Karlsruhe, 1996.
[35] H. Fesefeldt, preprint PITHA-85/02, RWTH Aachen, 1985.
[36] M. Bleicher et al., J. Phys. G: Nucl. Part. Phys. 25 (1999) 1859.
[37] A. Mücke et al., Comput. Phys. Commun. 124 (2000) 290, astro-ph/9903478.
[38] H.J. Drescher et al., Astropart. Phys. 21 (2004) 87, astro-ph/0307453.
[39] C. Meurer et al., Czech. J. Phys. 56 (2006) A211, astro-ph/0512536.
[40] P.D.B. Collins, *An Introduction to Regge Theorie & High Energy Physics* (Cambridge University Press, Cambridge, 1977).
[41] V.N. Gribov, Sov. Phys. JETP 26 (1968) 414.
[42] N.N. Kalmykov and S.S. Ostapchenko, Phys. Atom. Nucl. 56 (1993) 346.
[43] N.N. Kalmykov, S.S. Ostapchenko, and A.I. Pavlov, Nucl. Phys. Proc. Suppl. 52B (1997) 17.
[44] S. Ostapchenko, Phys. Rev. D 74 (2006) 014026, hep-ph/0505259.
[45] S. Ostapchenko, Phys. Lett. B 636 (2006) 40, hep-ph/0602139.
[46] J. Engel et al., Phys. Rev. D 46 (1992) 5013.
[47] R.S. Fletcher et al., Phys. Rev. D 50 (1994) 5710.
[48] R. Engelet al., Proceedings of the 26th ICRC, Salt Lake City, Utah, 1999, p. 415.
[49] K. Werner, F.-M. Liu, and T. Pierog, Phys. Rev. C 74 (2006) 044902, hep-ph/0506232.
[50] T. Pierog and K. Werner, *New facts about muon production in Extended Air Shower simulations*, arXiv:0611311v1[astro-ph].
[51] T. Pierog and K. Werner, Proceedings of the 30th ICRC, Mérida, México, 2007, Vol. 4, p. 629.
[52] J. Ranft, Phys. Rev. D 51 (1995) 64.
[53] S. Roesler, R. Engel, and J. Ranft, Prepared for the 27th ICRC, Hamburg, Germany, 2001, p. 439.
[54] F.W. Bopp et al., Phys. Rev. C 77 (2008) 014904; F.W. Bopp et al., *Antiparticle to Particle Production Ratios in Hadron-Hadron and d-Au Collisions in the DPMJET-III Monte Carlo*, hep-ph/0505035v2.
[55] M. Zha, J. Knapp, and S. Ostapchenko, Prepared for the 28th ICRC, Tsukuba, Japan, 2003, p. 515.
[56] R. Engel, Nucl. Phys. Proc. Suppl. 122 (2003) 40.
[57] J. Linsley and A.A. Watson, Phys. Rev. Lett. 46 (1981) 459.
[58] J. Alvarez-Muniz et al., Phys. Rev. D 66 (2002) 033011, astro-ph/0205302.
[59] L. Anchordoqui et al., Ann. Phys. 314 (2004) 145, hep-ph/0407020.
[60] B.R. Dawson, R. Meyhandan, and K.M. Simpson, Astropart. Phys. 9 (1998) 331, astro-ph/9801260.
[61] M. Ave et al., Astropart. Phys. 19 (2003) 61, astro-ph/0203150.
[62] M.T. Dova et al., *New constraints on the mass composition of cosmic rays above* 10^17 *eV from Volcano Ranch measurements*, arXiv:0312463v1[astro-ph].
[63] M. Ave et al., Prepared for the 28th ICRC, Tsukuba, Japan, 2003, p. 349.

[64] K. Shinozaki et al. (AGASA Collaboration), Prepared for the 28th ICRC, Tsukuba, Japan, 2003, p.401.
[65] R.U. Abbasi et al.(The High Resolution Fly's Eye Collaboration), Astrophys. J. 622 (2005) 910, astro-ph/0407622.
[66] J. Matthews, Astropart. Phys. 22 (2005) 387.
[67] R. Engel (Auger Collaboration), Proceedings of the 30th ICRC, Mérida, México, 2007, Vol. 4, p. 385.
[68] J.R. Hörandel, J. Phys. G 29 (2003) 2439, astro-ph/0309010.
[69] T. Abu-Zayyad et al. (HiRes Collaboration), Nucl. Instrum. Meth. A 450 (2000) 253.
[70] A.S. Chou et al. (Pierre Auger Collaboration), Proceedings of the 29th ICRC, Pune, India, 2005, p. 319.
[71] F. Schmidt et al., *A Model-Independent Method of Determining Energy Scale and Muon Number in Cosmic Ray Surface Detectors*, arXiv:0712.3750[astro-ph].
[72] F. Schmidt et al., Proceedings of the 30th ICRC, Mérida, México, 2007, Vol. 4, p. 601.
[73] S. Ostapchenko, Czech. J. Phys. 56 (2006) A149, hep-ph/0601230.
[74] T. Sanuki et al., Phys. Rev. D 75 (2007) 043005, astro-ph/0611201.
[75] V. Avati et al., Astropart. Phys. 19 (2003) 513.
[76] J. Abdallah et al. (DELPHI Collaboration), Astropart. Phys. 28 (2007) 273, 0706.2561.
[77] Y. Ma et al., Proceedings of the 30th ICRC, Mérida, México, 2007, Vol. 5, p. 1213.
[78] X. Bai et al. (AMANDA Collaboration), Proceedings of the 28th ICRC, Tsukuba, Japan, 2003, p. 1373.
[79] J. Ridky et al., Proceedings of the 30th ICRC, Mérida, México, 2007, Vol. 4, p. 605.
[80] H. Ulrich et al., Czech. J. Phys. 56 (2006) A261.
[81] S.K. Gupta et al. (GRAPES Collaboration), Proceedings of the 30th ICRC, Mérida, México, 2007, Vol. 5, p. 1121.
[82] H. Tanaka et al. (GRAPES Collaboration), Proceedings of the 30th ICRC, Mérida, México, 2007, Vol. 4, p. 55.
[83] H. Tanaka et al. (GRAPES Collaboration), Proceedings of the 30th ICRC, Mérida, México, 2007, Vol. 4, p. 691.
[84] H.J. Drescher et al., Phys. Rept. 350 (2001) 93; and hep-ph/0007198.
[85] V.N. Gribov, M.L. Levin, and M.G. Ryskin, Phys. Rep. 100 (1983) 1.
[86] T. Pierog et al., Proceedings of the 30th ICRC, Mérida, México, 2007, Vol. 4, p. 625.
[87] P.K.F. Grieder, Proceedings of the 13th ICRC, Denver, 1973.
[88] H.-J. Drescher, Phys. Rev. D 77 (2007) 056003, arXiv:0712.1517 [hep-ph].
[89] H. Ulrich (KASCADE Collaboration), Proceedings of the 30th ICRC, Mérida, México, 2007, Vol. 4, p. 87.
[90] N. Armesto et al., Phys. Lett. B 344 (1995) 301.
[91] N. Armesto et al., Astropart. Phys. 6 (1997) 327.
[92] M.A. Braun and C. Pajares, Phys. Rev. Lett. 85 (2000) 4864, hep-ph/0007201.
[93] M.A. Braun et al., Eur. Phys. J. C 25 (2002) 249, hep-ph/0111378.
[94] M.A. Braun et al., Eur. Phys. J. C 32 (2004) 535, hep-ph/0307056.
[95] P. Brogueira and J. Dias de Deus, Phys. Rev. C 72 (2005) 044903, hep-ph/0506081.
[96] P. Brogueira, J. Dias de Deus, and C. Pajares, Phys. Rev. C 75 (2007) 054908, hep-ph/0605148.
[97] L. Cunqueiro, J. Dias de Deus, E. G. Ferreiro, and C. Pajares, Eur. Phys. J. C 53 (2008) 585, hep-ph/0712.0509.
[98] N. Armesto, C. Pajares, and D. Sousa, Phys. Lett. B 527 (2002) 92, hep-ph/0104269.
[99] M.A. Braun, F. Del Moral, and C. Pajares, Phys. Rev. C 65 (2002) 024907, hep-ph/0105263.
[100] C. Pajares, D. Sousa, and R.A. Vázquez, Phys. Rev. Lett. 89 (2001) 1674.
[101] J. Dias de Deus et al., Phys. Rev. Lett. 96 (2006) 162001; and hep-ph/0507227.
[102] C. Pajares, D. Sousa, and R.A. Vazquez, Astropart. Phys. 12 (2000) 291.
[103] V. Canoa et al., Astropart. Phys. 23 (2005) 435, astro-ph/0409619.
[104] J. Alvarez-Muniz et al., Astropart. Phys. 27 (2007) 271, hep-ph/0608050.
[105] J. Alvarez-Muñiz et al., Proceedings of the 30th ICRC, Mérida, México, 2007, Vol. 4,

p. 659.
[106] R. Ulrich et al., *On the measurement of the proton-air cross section using cosmic ray data*, arXiv:0709.1392[astro-ph]; R. Ulrich et al., Proceedings of 12th Int. Conf. on Elastic and Diffractive Scattering, Hamburg, 2007.
[107] N.L. Grigorov et al., Proceedings of the 9th ICRC, London, England, 1965, Vol. 1, p. 860.
[108] G.B. Yodh, Y. Pal, and J.S. Trefil, Phys. Rev. Lett. 28 (1972) 1005.
[109] R.A. Nam et al., Proceedings of the 14th ICRC, Munich, 1975, Vol.7, p. 2258.
[110] F. Siohan et al., J. Phys. G 4 (1978) 1169.
[111] H.H. Mielke et al., J. Phys. G 20 (1994) 637.
[112] R.M. Baltrusaitis et al., (Fly's Eye Collaboration), Phys. Rev. Lett. 52 (1984) 1380.
[113] M. Honda et al., (AGASA Collaboration), Phys. Rev. Lett. 70 (1993) 525.
[114] M. Aglietta et al. (EAS-TOP Collaboration), Proceedings of the 26th ICRC, Salt Lake City, Utah, 1999, Vol. 1, p. 143.
[115] T. Hara et al., Phys. Rev. Lett. 50 (1983) 2058.
[116] S.P. Knurenko et al., Proceedings of the 26th ICRC, Salt Lake City, Utah, 1999, Vol. 1, p. 372.
[117] K. Belov (HiRes Collaboration), Nucl. Phys. Proc. Suppl. 151 (2006) 197.
[118] L. N. Lipatov, Phys. Rept. 286 (1997) 131, hep-ph/9610276.
[119] L. Frankfurt, M. Strikman, and C. Weiss, Ann. Rev. Nucl. Part. Sci. 55 (2005) 403, hep-ph/0507286.
[120] H. J. Drescher and M. Strikman, Phys. Rev. Lett. 100 (2008) 152002, arXiv:0712.3209 [hep-ph].
[121] K. Belov (HiRes Collaboration), Proceedings of the 30th ICRC, Mérida, México, 2007, Vol. 4, p. 687.
[122] I. De Mitri (ARGO-YBJ Collaboration), Proceedings of the 30th ICRC, Mérida, México, 2007, Vol. 4, p. 675.
[123] G. C. Trinchero (EAS-TOP Collaboration), Proceedings of the 30th ICRC, Mérida, México, 2007, Vol. 4, p. 27.
[124] R. Ulrich et al., Proceedings of the 30th ICRC, Mérida, México, 2007, Vol. 4, p. 679.
[125] C. Meurer et al. (HARP Collaboration), Proceedings of the 30th ICRC, Mérida, México, 2007, Vol. 4, p. 683.
[126] M.G. Catanesi et al. (HARP Collaboration), *Measurement of the production cross-sections of $\pi^{\pm}$ in p-C and $\pi^{\pm}$-C interactions at 12 GeV/c*, arXiv:0802.0657[astro-ph].
[127] R.J. Glauber and G. Matthiae, Nucl. Phys. B 21 (1970) 135.
[128] J.H. Weis, Acta Physica Polonica B 7 (1976) 851.
[129] T.K. Gaisser et al., Phys. Rev. D 54 (1996) 5578, hep-ph/9608253.
[130] M. Honda et al., Phys. Rev. D 75 (2007) 043006, astro-ph/0611418.
[131] G. Maier and J. Knapp, Proceedings of the 30th ICRC, Mérida, México, 2007, Vol. 4, p. 597.
[132] G. Maier and J. Knapp, Astropart. Phys. 28 (2007) 72, arXiv:0704.3567 [astro-ph].
[133] T.K. Gaisser and M. Honda, Ann. Rev. Nucl. Part. Sci. 52 (2002) 153, hep-ph/0203272.
[134] G. Barr and R. Engel, Nucl. Phys. Proc. Suppl. 151 (2006) 175; and astro-ph/0504356; to appear in Proc. of 13th Int. Symposium on Very High-Energy Cosmic Ray Interactions, Pylos, Greece, 2004.
[135] C. Alt et al. (NA49 Collaboration), Eur. Phys. J. C 49 (2007) 897, hep-ex/0606028.
[136] G. Barr et al., Eur. Phys. J. C 49 (2007) 919, hep-ex/0606029.
[137] M.G. Catanesi et al. (HARP Collaboration), Nucl. Instrum. Meth. A 571 (2007) 527.
[138] S. Afanasev et al. (NA49 Collaboration), Nucl. Instrum. Meth. A 430 (1999) 210.
[139] C. Meurer et al. (HARP Collaboration), *New p+C data in fixed target experiments and the muon component in extensive air showers*, arXiv:0612157v1[astro-ph].
[140] A. Laszlo et al. (NA61 Collaboration), *Na61/Shine at the CERN SPS*, arXiv:0709.1867[nucl-ex]; Proc of 4th International Workshop Critical Point and Onset of Deconfinement, Darmstadt, 2007.
[141] K. Kaneyuki (T2K Collaboration), Nucl. Phys. Proc. Suppl. 145 (2005) 178.
[142] R. Raja (MIPP Collaboration), Pramana 67 (2006) 951.

[143] H. Menjo (LHCf Collaboration), Proceedings of the 30th ICRC, Mérida, México, 2007, Vol. 5, p. 1097.
[144] H. Menjo (LHCf Collaboration), Proceedings of the 30th ICRC, Mérida, México, 2007, ID 0981.
[145] T. Sako et al., Nucl. Instrum. Meth. A 578 (2007) 146.
[146] G. Anelli et al. (TOTEM Collaboration), *TOTEM Physics*, hep-ex/0602025.
[147] A.L.S. Angelis et al., Nuovo Cim. 24 C (2001) 755.
[148] M. Albrow et al. (CMS and TOTEM Collaboration), CERN-LHCC-2006-039, CMS Note-2007/002, TOTEM Note 06-5.
[149] A.M. Hillas, Proceedings of the 17th ICRC, Paris, France, 1981, p. 193.
[150] G. Rubtsov et al., Proceedings of the 30th ICRC, Mérida, México, 2007, Vol. 4, p. 637.
[151] D. S. Gorbunov, G. I. Rubtsov, and S. V. Troitsky, Phys. Rev. D 76 (2007) 043004, astro-ph/0703546.
[152] H.-J. Drescher and G. R. Farrar, Phys. Rev. D 67 (2003) 116001, astro-ph/0212018.
[153] T. Bergmann et al., Astropart. Phys. 26 (2007) 420, astro-ph/0606564.
[154] J. Allen and G. Farrar, Proceedings of the 30th ICRC, Mérida, México, 2007, Vol. 4, p. 645.
[155] K. Kasahara, Proceedings of the 30th ICRC, Mérida, México, 2007, Vol. 4, p. 581.
[156] F. Cohen and K. Kasahara, Proceedings of the 30th ICRC, Mérida, México, 2007, Vol. 4, p. 585.
[157] H. Falcke (LOPES Collaboration), Proceedings of the 30th ICRC, Mérida, México, 2007, Vol. 6, p. 79.
[158] G. Bertone, D. Hooper, and J. Silk, Phys. Rept. 405 (2005) 279, hep-ph/0404175.
[159] V. Berezinsky, M. Kachelriess, and S. Ostapchenko, Phys. Rev. Lett. 89 (2002) 171802, hep-ph/0205218.
[160] J. F. Beacom, N. F. Bell, and G. D. Mack, Phys. Rev. Lett. 99 (2007) 231301, astro-ph/0608090.
[161] M. Kachelriess and P. D. Serpico, Proceedings of the 30th ICRC, Mérida, México, 2007, Vol. 4, p. 701.
[162] H. Yuksel et al., Phys. Rev. D 76 (2007) 123506,arXiv:0707.0196[astro-ph].
[163] G. D. Mack et al.,*Conservative Constraints on Dark Matter Annihilation into Gamma Rays*, arXiv:0803.0157[astro-ph].
[164] Q. Yuan and X. Y. Bi, Proceedings of the 30th ICRC, Mérida, México, 2007, Id 0034.
[165] L. Pieri et al., Proceedings of the 30th ICRC, Mérida, México, 2007, Vol. 4, p. 725.
[166] C. Giocoli, L. Pieri, and G. Tormen, Proceedings of the 30th ICRC, Mérida, México, 2007, Vol. 4, p. 757.
[167] W. de Boer and V. Zhukov, Proceedings of the 30th ICRC, Mérida, México, 2007, Vol. 4, p. 697.
[168] N. Fornengo et al., Proceedings of the 30th ICRC, Mérida, México, 2007, Vol. 4, p. 705.
[169] F. Donato et al., Proceedings of the 30th ICRC, Mérida, México, 2007, Vol. 4, p. 717.
[170] R. Aloisio, P. Blasi, and A. V. Olinto, Astrophys. J. 601 (2004) 47, astro-ph/0206036.
[171] L. Bergstrom, Rept. Prog. Phys. 63 (2000) 793, hep-ph/0002126.
[172] D. Hubert et al. (ICECUBE Collaboration), Proceedings of the 30th ICRC, Mérida, México, 2007, Vol. 4, p. 709.
[173] E. Moulin et al. (H.E.S.S. Collaboration), Proceedings of the 30th ICRC, Mérida, México, 2007, Vol. 4, p. 713.
[174] M. Doro *et al.* (MAGIC Collaboration), Proceedings of the 30th ICRC, Mérida, México, 2007, Vol. 4, p. 721.
[175] L. S. Stark et al. (MAGIC Collaboration), Proceedings of the 30th ICRC, Mérida, México, 2007, Vol. 4, p. 745.
[176] S. Schael et al. (AMS Collaboration), Proceedings of the 30th ICRC, Mérida, México, 2007, Vol. 4, p. 753.
[177] J. Alcaraz et al. (AMS Collaboration), Phys. Lett. B 484 (2000) 10.
[178] R. L. Golden et al. (WIZARDS Collaboration), Astrophys. J. 457 (1996) L103.
[179] J. J. Beatty et al., Phys. Rev. Lett. 93 (2004) 241102, astro-ph/0412230.
[180] I. V. Moskalenko and A. W. Strong, Astrophys. J. 493 (1998) 694, astro-ph/9710124.
[181] W. de Boer et al., Astron. Astrophys. 444 (2005) 51, astro-ph/0508617.
[182] L. Bergstrom et al., JCAP 0605 (2006) 006, astro-ph/0602632.

[183] V. I. Yakovlev et al., Proceedings of the 30th ICRC, Mérida, México, 2007, Id 0021.

[184] J. Cook et al., Proceedings of the 30th ICRC, Mérida, México, 2007, Vol. 4, p. 825.

[185] S. Cecchini et al., Proceedings of the 30th ICRC, Mérida, México, 2007, Vol. 4, p. 787.

[186] H. Wissing et al. (ICECUBE Collaboration), Proceedings of the 30th ICRC, Mérida, México, 2007, Vol. 4, p. 799.

[187] A. Pohl et al. (ICECUBE Collaboration), Proceedings of the 30th ICRC, Mérida, México, 2007, Vol. 4, p. 803.

[188] F. Z. Mohammed Sahnoun et al., Proceedings of the 30th ICRC, Mérida, México, 2007, Id 0636.

[189] P. A. M. Dirac, Proc. Roy. Soc. Lond. A 133 (1931) 60.

[190] A. M. Polyakov, JETP Lett. 20 (1974) 194.

[191] G. 't Hooft, Nucl. Phys. B 79 (1974) 276.

[192] V. Aynutdinov et al. (Baikal Collaboration), *Search for relativistic magnetic monopoles with the Baikal neutrino telescope NT200*, arXiv:0507713[astro-ph]; Proceedings of the 29th ICRC, Pune, India, 2005.

[193] M. Ambrosio et al. (MACRO Collaboration), Eur. Phys. J. C25 (2002) 511, hep-ex/0207020.

[194] V. A. Rubakov, Nucl. Phys. B 203 (1982) 311.

[195] B. Christy et al. (ICECUBE Collaboration), Proceedings of the 30th ICRC, Mérida, México, 2007, Vol. 4, p. 795.

[196] S. Rosier Lees et al. (AMS Collaboration), Proceedings of the 30th ICRC, Mérida, México, 2007, Vol. 4, p. 729.

[197] V. Choutko et al. (AMS Collaboration), Proceedings of the 30th ICRC, Mérida, México, 2007, Vol. 4, p. 765.

[198] A. Morselli et al. (GLAST LAT Collaboration), Proceedings of the 30th ICRC, Mérida, México, 2007, Vol. 4, p. 733.

[199] E. Nuss et al. (GLAST LAT Collaboration), Proceedings of the 30th ICRC, Mérida, México, 2007, Vol. 4, p. 737.

[200] G. Wikström et al. (ICECUBE Collaboration), Proceedings of the 30th ICRC, Mérida, México, 2007, Vol. 4, p. 741.

[201] J. E. Koglin et al., Proceedings of the 30th ICRC, Mérida, México, 2007, Vol. 4, p. 769.

[202] K. Yoshida et al., Proceedings of the 30th ICRC, Mérida, México, 2007, Vol. 4, p. 817.